有机化学 DOI: 10.6023/cjoc202108025 研究论文
Chinese Journal of Organic Chemistry ARTICLE

紫精寡聚体的水相折叠和堆积及葫芦[*n*]脲(*n*＝7, 8)调控

彭文昶[a] 王 辉[a] 张丹维*,[a] 黎占亭*,[a,b]
([a]复旦大学化学系 上海市分子催化和功能材料重点实验室 上海 200438)
([b]中国科学院上海有机化学研究所 有机功能分子合成与组装化学重点实验室 上海 200032)

摘要 为探索紫精正离子自由基线性分子的水相构象和簇集, 制备了一系列具有不同长度和连接基团的水溶性紫精寡聚体. 重水中 ^{1}H NMR 实验显示, 在水中葫芦[7]脲(CB[7])及葫芦[8]脲(CB[8])包结其对-二甲基苯单元而不是联吡啶单元. 紫外可见吸收实验表明, 在连二亚硫酸钠水溶液中, 线性分子的紫精基团被还原为相应的正离子自由基, 分子骨架通过折叠发生堆积形成褶皱型二聚体, 并导致自由基堆积三聚体络合物的形成. 动态光散射实验揭示, 这些自由基受疏水作用驱动通过折叠构象形成稳定的二聚体, 再进一步堆积形成纳米尺寸的簇集体. 加入葫芦[7]脲导致这些折叠体的紫精正离子自由基与葫芦[7]脲形成 1∶1 包结络合物, 从而诱导纳米簇集结构解聚. 而 CB[8]也可以通过与紫精正离子自由基形成 1∶2 包结络合物, 促使纳米簇集体和折叠体的解聚. 在线性分子中引入刚性连接基团可以进一步促进其正离子自由基的堆积. 尽管线性紫精正离子自由基结构在乙腈中堆积形成折叠体二聚体文献已有报道, 本项研究揭示这类分子在水中的堆积进一步增强, 其折叠体二聚体可以进一步堆积, 形成纳米尺度的簇集体.
关键词 折叠; 簇集; 自由基正离子; 葫芦[*n*]脲(*n*＝7, 8); 4,4'-二吡啶盐; 水相

Folding and Aggregation of Oligoviologens in Water and Cucurbit[*n*]uril (*n*＝7, 8) Modulation

Peng, Wen-Chang[a] Wang, Hui[a] Zhang, Dan-Wei*,[a] Li, Zhan-Ting*,[a,b]
([a] *Shanghai Key Laboratory of Molecular Catalysis and Innovative Materials*, *Department of Chemistry*, *Fudan University*, *Shanghai 200438*)
([b] *Key Laboratory of Synthetic and Self-Assembly Chemistry for Organic Functional Molecules*, *Shanghai Institute of Organic Chemistry*, *Chinese Academy of Sciences*, *Shanghai 200032*)

Abstract To study the conformations and aggregation of linear viologen radical cation-incorporated molecules in water, a series of water-soluble oligoviologens with different length and linkers were prepared. ^{1}H NMR experiments in deuteroxide showed that cucurbit[7]uril (CB[7]) and cucurbit[8]uril (CB[8]) encapsulate their *p*-xylylene linkers instead of the bipyridinium units. UV-vis absorption experiments indicated that in the aqueous solution of sodium dithionite the viologen units of the oligomers were reduced to the radical cation species which were driven to dimerize through pleated conformations, leading to the formation of trisradical cation species. Dynamic light scattering experiments revealed that the foldamer dimers further aggregated to afford nanoscale particles. Adding CB[7] decomposed all the aggregated foldamer nanoparticles through 1∶1 encapsulation of the viologen radical cation units, whereas the addition of CB[8] broke the foldamers and their large aggregates through 1∶2 encapsulation of the viologen radical cations. Introducing a rigid linker to the linear viologen molecule could further enhance their stacking in the radical cation state. Although the folding and dimerization of linear viologen radical cation molecules have been established in acetonitrile in the literature, this study demonstrates that in water such multiple viologen radical cation molecules not only undergo folding to form stable dimers, but also further aggregate to give rise to nanoscale particles.
Keywords folding; aggregation; radical cation; cucurbit[*n*]uril (*n*＝7, 8); 4,4'-bipyridinium; aqueous medium

* Corresponding authors. E-mail: zhangdw@fudan.edu.cn, ztli@fudan.edu.cn
Received August 17, 2021; revised October 27, 2021; published online November 3, 2021.
Project supported by the National Natural Science Foundation of China (Nos. 21890732, 21890730, 21921003).
国家自然科学基金(Nos. 21890732, 21890730, 21921003)资助项目.

1 Introduction

Folding and aggregation are two common behaviours of linear molecules, which may, to a considerable extent, modulate their special properties. The driving forces may be intrinsic non-covalent interactions possessed by the molecules or solvophobicity in solution. Peptides and proteins are the most important biomacromolecules that can be induced mainly by hydrogen bond and hydrophobicity to fold into helical, sheet or turn secondary structures and further aggregate into more advanced tertiary structures stabilized by discrete intra- and intermolecular interactions.[1-2] Achieving a better understanding and regulation of the relationship between intra- and intermolecular interactions could help to unravel the rules governing the formation of the advanced structures of biomacromolecules and also create synthetic structures that exhibit new properties or functions unavailable for natural molecules. Inspired by the formation of discrete secondary structures of biomacromolecules, in the past decades, chemists have designed and constructed a large variety of foldamers using synthetic backbones.[3] Among others, aromatic foldamers have been revealed to exhibit versatile functions including, such as, molecular recognition[3-4] and transmembrane channels.[5] Aromatic foldamers with conformational switching have also been reported.[6] However, examples of linear aromatic molecules that adopt a folded conformation in aqueous media are relatively limited,[7] whereas the development of efficient methods to tune the folding of aromatic backbones has not been explored. Given that life exists in water where hydrophobicity is expected to always impose an important influence on the folding and aggregation of linear molecules that are not fully hydrophilic, it would be of importance to study the aqueous-phase folding and modulation of aromatic molecules that have been established to form a well-defined compact conformation in organic solvents.

We and others have reported that oligo- and polyviologens can be induced by strong intramolecular radical-radical interactions to fold into pleated conformations when the 4,4'-bipyridinium ($BIPY^{2+}$) units incorporated in the backbones are reduced to the corresponding radical cationic forms, namely, $BIPY^{\bullet+}$-in acetonitrile.[8-9] Different from other driving forces such as hydrogen bonding, this radical-radical interaction of $BIPY^{\bullet+}$can exhibit di- and triradical complexation motifs,[10-11] which depends on the structures and lengths of the backbones. Because it has been established that this radical-radical interaction is enhanced in aqueous media,[12] we were interested in investigating the folding and aggregation of linear viologen molecules in water. Herein we report the folding and aggregation properties of two linear molecules that contain two or three $BIPY^{\bullet+}$ units in water and the modulation of cucurbit[*n*]urils (*n*=7,8) for both processes.

2 Results and discussion

Three $BIPY^{2+}$ derivatives **1V**•2Cl, **2V**•4Cl and **3V**•6Cl were used for the interaction of their $BIPY^{\bullet+}$unit(s) in the reduced state (Scheme 1). The tetra- and hexacationic compounds were first prepared as PF_6^- salt according to the reported methods,[9,13] which was converted to the water-soluble Cl^- salt through anion exchange. The encapsulation patterns of the three compounds by CB[7] and CB[8] were first investigated using ^{1}H NMR titration experiments in D_2O. These two rigid macrocycles have been demonstrated to encapsulate hydrophobic aromatic guests to generate a variety of supramolecular architectures.[14] As expected, **1V**•2Cl formed a 1∶1 complex with either of the macrocycles,[15-16] as the *β*-H signal of its viologen unit underwent upfield shifting to reach the maximum ($\Delta\delta$ −1.55 and −0.95, respectively) with the addition of 1.0 equiv. of the macrocycles (Supporting Information, Figures S1 and S2). ^{1}H NMR titration experiments in D_2O showed that **2V**•4Cl also formed a 1∶1 complex with the two macrocycles. However, the macrocycle preferred to encapsulate hydrophobic benzene ring because both the C**H** signal of the benzene ring and the C**H**$_2$ signal suffered the largest upfield shifting ($\Delta\delta$ −1.00 and −0.42 for CB[7], −0.78 and −0.42 for CB[8], respectively) (Supporting Information, Figures S3 and S4),[17] even though the *α*- and *β*-H signals of the viologen units also gave rise to observable shifting. This result was consistent with the fact that the benzene ring is more hydrophobic than the dicationic viologen unit. ^{1}H NMR experiments also indicated that both CB[7] and CB[8] preferred to encapsulate the *p*-xylene units of **3V**•6Cl to afford 1∶2 complexes when 2.0 equiv. or more amounts of the macrocycle were added (Supporting Information, Figures S5 and S6). For CB[7], this 1∶2 complex caused the benzene C**H** signal to upfield shift to δ 6.63, where two doublets overlapped partially, from δ 7.66. However, when 0.3～1.8 equiv. of CB[7] was added, another signal of the C**H** proton was also observed at δ 6.88, which became stronger firstly and then weaker, and finally disappeared after 2.0 equiv. of CB[7] was added. This signal was thus ascribed to that of the 1∶1 complex. Throughout the addition of CB[7], this signal was weaker than that of the 1∶2 complex, which implied that the two CB[7] rings of the 1∶2 complex might undergo intra- and/or intermolecular stacking to stabilize the two 1∶1 complexes of the same 1∶2 complex. For the case of CB[8], its addition originally led to the formation of the 1∶1 complex, as indicated by the occurrence of the single signal at δ 7.22. With the increase of CB[8], this signal became continually weaker and finally disappeared. Accompanied with the weakening of this signal, two doublets were formed at δ 7.17 and 6.90, which supported the formation of the 1∶2 complex and also reflected that the encapsulation of the benzene rings by CB[8] differentiated the chemical environments of their two pairs of protons. Dynamic light scattering (DLS) experiments revealed that, in the absence and presence of CB[7] or CB[8], the solution of the three viologen derivatives (0.20 mmol/L) did not give rise to large aggregates, with hydrodynamic diameter (D_H) being determined to be

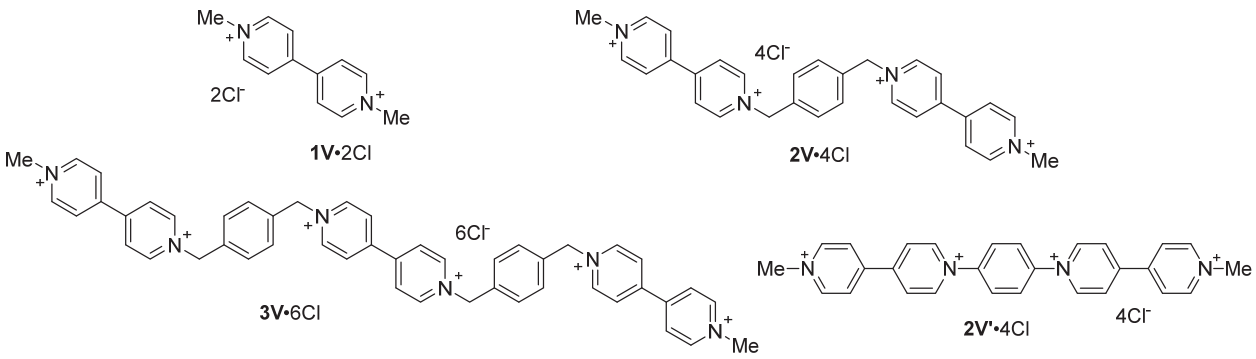

Scheme 1 Structures of compounds **1V**•2Cl, **2V**•4Cl, **3V**•6Cl and **2V'**•4Cl

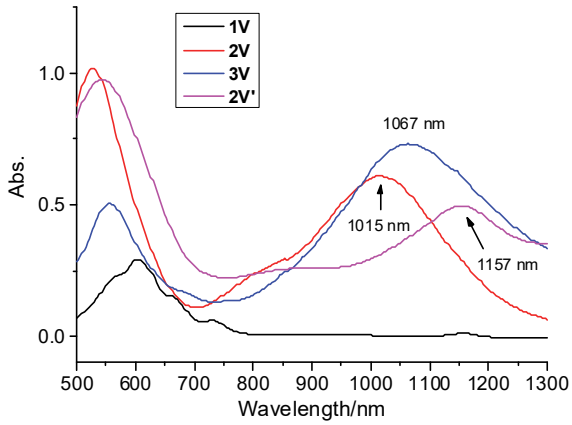

Figure 1 UV-vis absorption spectra of compounds **1V**•2Cl, **2V**•4Cl, **3V**•6Cl and **2V4'**•Cl ([BIPY]=0.20 mmol/L) in water containing sodium dithionite (0.10 mol/L), which reduces their $BIPY^{2+}$ unit(s) to $BIPY^{\bullet+}$ at 25 ℃

⩽2 nm, indicating that these multicationic compounds did not undergo important stacking.

The stacking properties of the molecules were then studied using UV-vis spectroscopy in water with the $BIPY^{2+}$ unit(s) being reduced to $BIPY^{\bullet+}$ by sodium dithionite (Figure 1).[12] In all the cases, excessive sodium dithionite was used to avoid the oxidation of $BIPY^{\bullet+}$ to $BIPY^{2+}$ by oxygen in air. The spectrum of the solution of $\mathbf{1V}^{\bullet+}$ displayed a strong absorption band around 603 nm, which is typical of that of the $BIPY^{\bullet+}$ monomer,[12] but no important absorption within the longer wavelength (>800 nm), reflecting that the radical cation did not dimerize to afford dimers of important concentration. The spectrum of the solution of $\mathbf{2V}^{2(\bullet+)}$ exhibited three absorption bands around 527, 837 and 1015 nm, respectively. The strong absorption band centered at 527 nm was produced by the $BIPY^{\bullet+}$monomers.[12] The distinct absorption band around 837 nm can be ascribed to the formation of radical-radical dimers $[BIPY^{\bullet+}]_2$,[11-12] while the one around 1015 nm can be assigned to the formation of triradical complexes $[BIPY^{\bullet+}]_3$ from three $BIPY^{\bullet+}$ units.[11,18] Similarly, the spectrum of the solution of $\mathbf{3V}^{3(\bullet+)}$ also exhibited three absorption bands which centered at 556, 852 and 1067 nm, respectively, which can also be ascribed to the formation of the $BIPY^{\bullet+}$ monomers, dimers and trimers. The wavelength of the absorption band of the trisradical complexes of $\mathbf{3V}^{3(\bullet+)}$ was distinctly longer than that of $\mathbf{2V}^{2(\bullet+)}$, which might reflect more compact stacking of the $BIPY^{\bullet+}$ monomers.[18]

The rigidity of the *p*-xylene linker(s) would not allow intramolecular stacking of the $BIPY^{\bullet+}$ units. Thus, the formation of the dimers and trimers of the $BIPY^{\bullet+}$ units should proceed through their intermolecular stacking. UV-vis dilution experiments revealed that the absorption of the $BIPY^{\bullet+}$ unit of $\mathbf{1V}^{\bullet+}$ was linearly correlated with their concentration, with a molar extinction coefficient (ε) of about 1500 $L\bullet mol^{-1}\bullet cm^{-1}$ (Supporting Information, Figure S7). With the addition of 1.0 equiv. of CB[7], the ε of $\mathbf{1V}^{\bullet+}$ (930 $L\bullet mol^{-1}\bullet cm^{-1}$) was still constant at different concentrations (Figure S8), indicating the formation of stable 1∶1 complex $\mathbf{1V}^{\bullet+}\subset$CB[7].[15] Adding 0.5 equiv. of CB[8] to the solution of $\mathbf{1V}^{\bullet+}$ led to the formation of the absorption band of the $[BIPY^{\bullet+}]_2$ dimers centered at 878 nm through the formation of the 2∶1 complex $(\mathbf{1V}^{\bullet+})_2\subset$CB[8] (Supporting Information, Figure S9).[16] DLS experiments showed that, at 0.28 mmol/L, the solution of $\mathbf{1V}^{\bullet+}$ showed the formation of very small particles with D_H being about 1.0 nm (Supporting Information, Figure S10). Adding 1.0 equiv. of CB[7] did not cause distinct change of the D_H, while its mixture with 0.5 equiv. of CB[8] gave rise to a D_H of about 2.7 nm. These results were consistent with the above UV-vis experiments and also indicated that the free radical cation, 1∶1 complex $\mathbf{1V}^{\bullet+}\subset$CB[7] and 2∶1 complex $(\mathbf{1V}^{\bullet+})_2\subset$CB[8] did not aggregate under the conditions used.

UV-vis experiments were then conducted for the solution of $\mathbf{2V}^{2(\bullet+)}$ in the absence and presence of CB[7] or CB[8]. Reducing its concentration from 0.14 to 0.02 mmol/L did not cause obvious decrease of the molar extinction coefficient of the trisradical complexes (ε=*ca.* 3000 $L\bullet mol^{-1}\bullet cm^{-1}$) which centered at 1013 nm (Figure 2a). Although the absorption of the diradical complexes (850 nm) could not be treated quantitatively due to overlapping with that of the trisradical complexes, this result supported that, within the concentration range investigated, $\mathbf{2V}^{2(\bullet+)}$ underwent intermolecular stacking through the same pattern. It was established that in acetonitrile $\mathbf{2V}^{2(\bullet+)}$ as hexafluorophoaphate salt adopted a folded conformation

which further stacked to form intertwined dimers as shown in Figure 3.[9] Given the fact that the stacking of the $BIPY^{\bullet+}$ units is stronger in water of more polarity, it is reasonable to propose that the molecules of $\mathbf{2V}^{2(\bullet+)}$ folded and stacked in the similar pattern. In the presence of 1.0 equiv. of CB[7], the absorption strength of the trisradical complexes was reduced remarkably, with the ε value of the absorption being reduced below 100 $L\bullet mol^{-1}\bullet cm^{-1}$ (Supporting Information, Figure S11). This result indicated that most of the intertwined dimers were decomposed due to the 1∶1 encapsulation of CB[7] for the $BIPY^{\bullet+}$ or *p*-xylene units of $\mathbf{2V}^{2(\bullet+)}$.[14] Adding 1.0 equiv. of CB[8] caused the absorption strength of the diradical complexes (850 nm) to disappear completely. Intriguingly, another absorption around 1010 nm maintained its ε (*ca.* 2300 $L\bullet mol^{-1}\bullet cm^{-1}$) unchanged at different concentrations (Figure 2b). Because CB[8] strongly encapsulates the $BIPY^{\bullet+}$ dimer in water, we proposed that this strong absorption centered at 1010 nm came from this dimer, which coincidently had a maximum absorption wavelength close to that of the triradical complex. With the incremental addition of CB[8], the shoulder peak of the dimer around 850 nm was decreased and finally vanished completely, whereas the strong absorption around 1013 nm also underwent obvious weakening. These observations should provide evidence for the encapsulation of the radical cations as stacking dimers (Supporting Information, Figure S12). The important bathochromic-shift of this diradical complex from 850 nm to 1010 nm might be tentatively attributed to its enhanced stability due to the encapsulation of CB[8].

UV-vis experiments were then further extended to the solution of $\mathbf{3V}^{3(\bullet+)}$ in the absence and presence of CB[7] or CB[8]. Within the concentration range of 0.01 mmol/L to 0.09 mmol/L, its UV-vis absorption spectra exhibited three absorption bands around 544, 860 and 1154 nm (Figure 2c), respectively, which can be ascribed to that of the monomers and stacked dimers and trimers of $BIPY^{\bullet+}$. The ε value of the trisradical complexes (2500 $L\bullet mol^{-1}\bullet cm^{-1}$) was also independent of the concentration. Previously, it has been demonstrated that the $\mathbf{3V}^{3(\bullet+)}$ molecules as hexafluorophosphate salt fold into pleated conformations in acetonitrile which further stack to afford stable intertwined dimers (Figure 3).[9] Thus, we propose that its stacking in water also takes place through a similar binding pattern with a pleated conformation. Adding 2.0 equiv. of CB[7] caused the absorption of the trisradical complexes to vanish nearly completely, which supports the decomposition of the trisradical complexes as a result of the encapsulation of CB[7] for the $BIPY^{\bullet+}$ or *p*-xylene units. With the addition of 1.5 equiv. of CB[8], the absorption of the trisradical complexes around 1150 nm was inhibited completely,

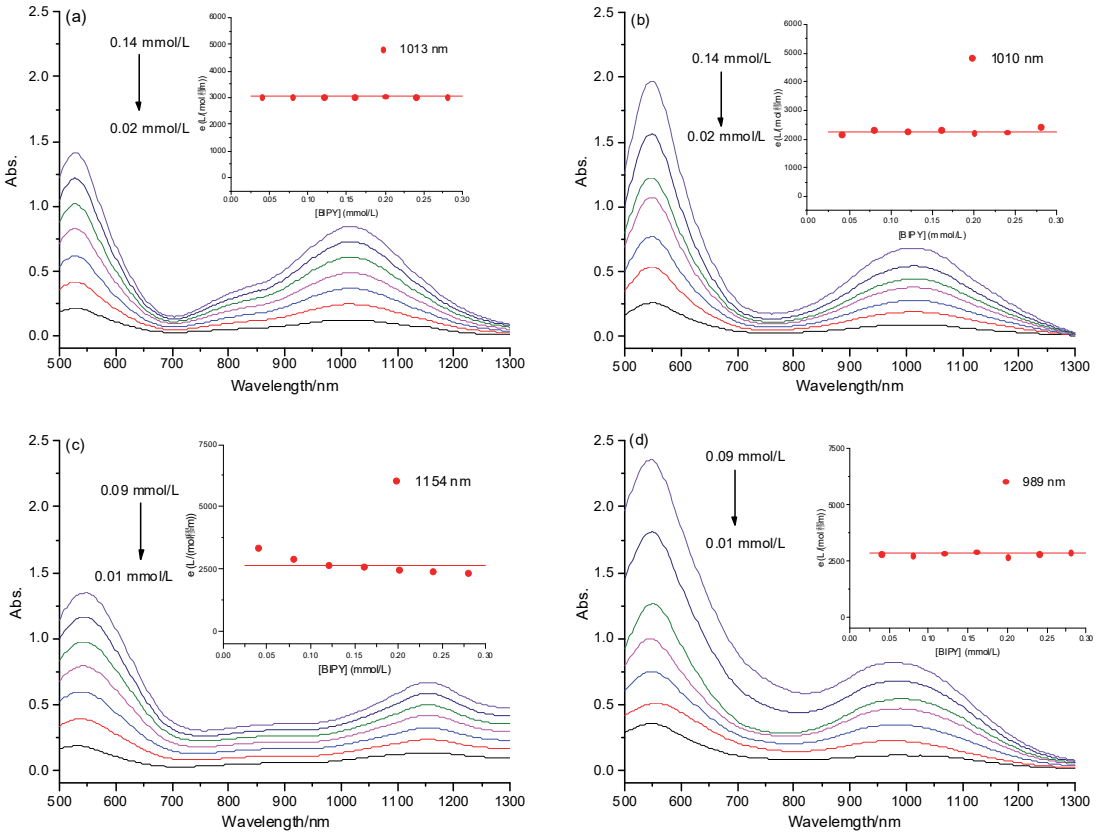

Figure 2 Absorption spectra of (a) $\mathbf{2V}^{2(\bullet+)}$ (0.02～0.14 mmol/L), (b) $\mathbf{2V}^{2(\bullet+)}$+1.0 equiv. CB[8] (0.02～0.14 mmol/L), (c) $\mathbf{3V}^{3(\bullet+)}$ (0.01～0.09 mmol/L) and (d) $\mathbf{3V}^{3(\bullet+)}$+1.5 equiv. CB[8] (0.01～0.09 mmol/L) in water containing sodium dithionite (50 mmol/L) (inset: the plot of ε of the absorption band around 1000 nm vs. [BIPY])

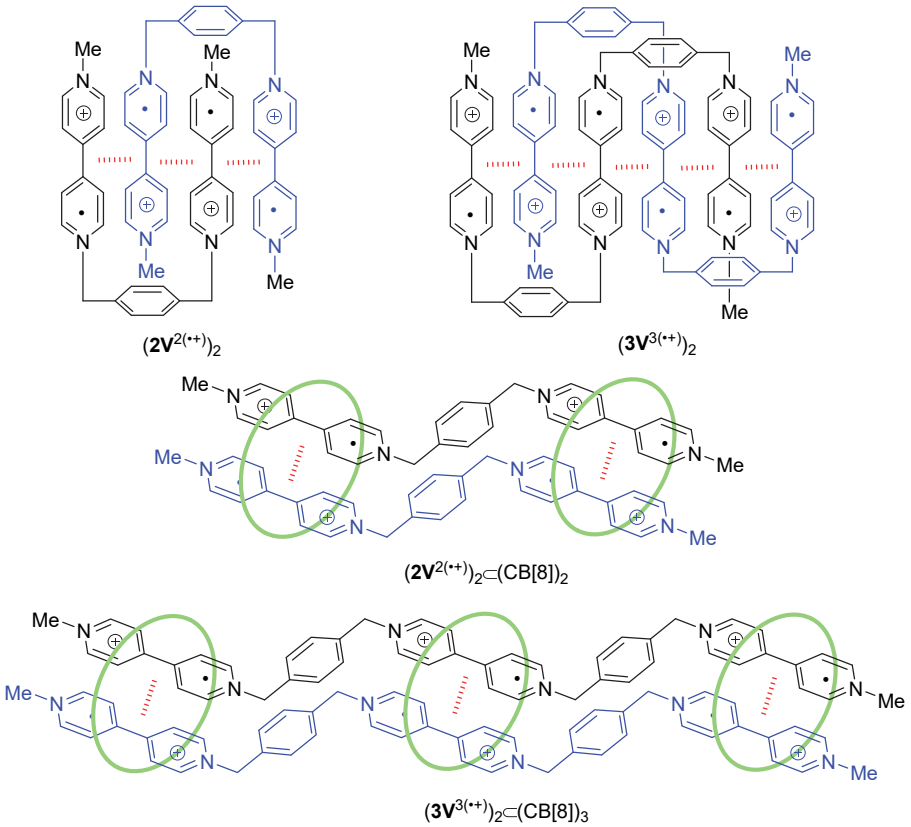

Figure 3 Tentative representation of the structures of pleated dimers $(2V^{2(\bullet+)})_2$ and $(3V^{3(\bullet+)})_2$ and encapsulation complexes $(2V^{2(\bullet+)})_2\subset(CB[8])_2$ and $(3V^{3(\bullet+)})_2\subset(CB[8])_3$

which was accompanied with the occurring of an absorption band around 990 nm (Figure 2d). These results supported the formation of CB[8]-encapsulated diradical complexes $(3V^{3(\bullet+)})_2\subset(CB[8])_3$ (Figure 3). The ε value of this absorption was determined to be 2500 L•mol^{-1}•cm^{-1}, which was unchanged when the concentration of **3V** was decreased from 0.09 mmol/L to 0.01 mmol/L, further confirming the high stability of such kind of multi-component encapsulation complexes.[19]

The aggregation of $1V^{\bullet+}$, $2V^{2(\bullet+)}$ and $3V^{3(\bullet+)}$ was further studied in water by DLS without or with the addition of CB[7] or CB[8] in water. The results are provided in Figure 4. As expected, the solution of $1V^{\bullet+}$ and its mixture with CB[7] (1∶1) or CB[8] (1∶0.5) all gave rise to a small peak with the D_H value being *ca.* 1 nm, which indicated that the radical cation and its 1∶1 and 2∶1 complexes did not further aggregate into larger particles. In contrast, the solution of $2V^{2(\bullet+)}$ showed the formation of large particles with an average D_H of 68 nm (Figure 4a). The above UV-vis absorption study already revealed that $2V^{2(\bullet+)}$ formed dimers through a pleated conformation. Thus, the formation of large particles in its solution suggested that the dimers should undergo strong stacking to form the large particles. Adding 1.0 equiv. of CB[7] led to the decomposition of these large particles and particles with average D_H of 1.3 nm were formed (Figure 4b), which was consistent with the above absorption study. That is, the two components formed 1∶1 encapsulation complexes which did not further stacked. Adding 1.0 equiv. of CB[8] led to the formation of larger particles with an average D_H of 74 nm (Figure 4c). Since the above absorption study revealed the formation of $(2V^{2(\bullet+)})_2\subset(CB[8])_2$ complexes, this result indicated that these multi-component complexes could further stack into large particles. Under similar conditions, the solution of $3V^{3(\bullet+)}$ afforded a D_H of 122 nm (Figure 4a). With the addition of 1.0 equiv. of CB[7], the D_H was reduced to 1.5 nm (Figure 4b). When 1.5 equiv. of CB[8] was added to the solution of $3V^{3(\bullet+)}$, the D_H was changed to 105 nm (Figure 4c). These results were very similar to those of $2V^{2(\bullet+)}$, reflecting that they underwent similar folding and stacking processes in water. Reducing the concentration also caused the decrease of the D_H value of the solution of $2V^{2(\bullet+)}$, $3V^{3(\bullet+)}$ and their mixture with CB[8]. At [BIPY]＝0.02 mmol/L, the value was determined to be 5, 7, 4 and 5 nm (Supporting Information, Figure S13), respectively. These results showed that at the low concentration, their pleated dimers and complexes $(2V^{2(\bullet+)})_2\subset(CB[8])_2$ and $(3V^{3(\bullet+)})_2\subset(CB[8])_3$ still aggregated into relatively large particles. These observations were in accordance with the above UV-vis absorption experiments, which revealed relatively constant ε values for the radical dimers and trimers.

To study the effect of the flexibility of the CH_2 linkers for the stacking of the $BIPY^{\bullet+}$ units, we further prepared compound **2V'**•4Cl and then reduced its $BIPY^{2+}$ units to two $BIPY^{\bullet+}$ radical cations using sodium dithionite. As

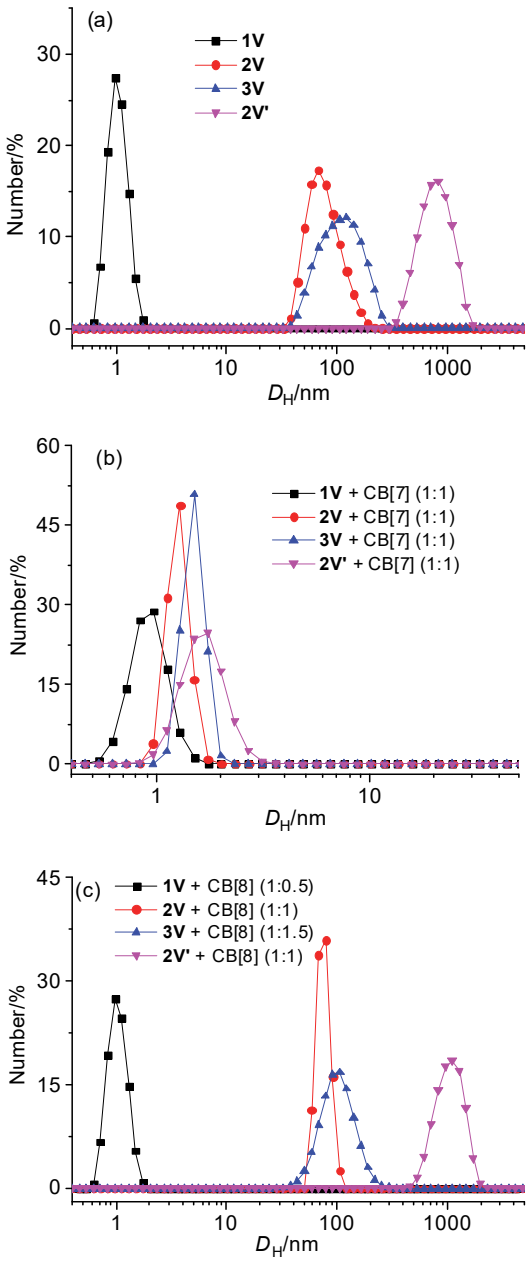

Figure 4 DLS profile of the solution of $\mathbf{1V}^{\bullet+}$, $\mathbf{2V}^{2(\bullet+)}$, $\mathbf{3V}^{3(\bullet+)}$ and $\mathbf{2V'}^{2(\bullet+)}$ in water containing sodium dithionite (50 mmol/L) in the (a) absence or presence of (b) CB[7] or (c) CB[8] ([BIPY]= 0.28 mmol/L)

expected, the solution of $\mathbf{2V'}^{2(\bullet+)}$ also displayed a strong absorption band centered at 1070 nm, which corresponded to the formation of stable trisradicals (Supporting Information, Figure S14a). Within the concentration range of 0.02 to 0.14 mmol/L, the ε value of this absorption was unchanged (3550 L•mol^{-1}•cm^{-1}), reflecting its high stability. Adding 1.0 equiv. of CB[7] to the solution of $\mathbf{2V'}^{2(\bullet+)}$ caused weakening of this absorption due to its encapsulation for the BIPY$^{\bullet+}$units of $\mathbf{2V'}^{2(\bullet+)}$ (Supporting Information, Figure S14b). Adding 1.0 equiv. of CB[8] led to the vanishing of this absorption of trisradical complexes, which was accompanied with remarkable enhancement of the absorption, centered at 890 nm, of radical dimers $[BIPY^{\bullet+}]_2$ as a results of strong encapsulation of CB[8] for the radical dimers to form $(\mathbf{2V'}^{2(\bullet+)})_2\subset(CB[8])_2$ complex (Supporting Information, Figure S14c). Again, the ε value of this absorption was roughly constant (3650 L•mol^{-1}•cm^{-1}) within the above concentration range. All these results were similar to those of $\mathbf{2V'}^{2(\bullet+)}$, supporting that they underwent similar stacking and binding patterns. DLS experiments revealed that the solution of $\mathbf{2V'}^{2(\bullet+)}$ (0.14 mmol/L) formed nanoparticles with an average D_H of 770 nm, which was substantially larger than that of $\mathbf{2V'}^{2(\bullet+)}$ of the same concentration, reflecting an enhanced stacking tendency (Supporting Information, Figure S15). However, with the addition of 1.0 equiv. of CB[7], the D_H was reduced to 1.7 nm, which indicated complete decomposition of the large particles due to the encapsulation of the BIPY$^{\bullet+}$ units by CB[7]. When 1.0 equiv. of CB[8] was added, the mixture formed even large particles, with the average D_H being determined to be 1100 nm, which, again, illustrated the high aggregating tendency of the corresponding complexes $(\mathbf{2V'}^{2(\bullet+)})_2\subset(CB[8])_2$. Diluting the concentration to 0.02 mmol/L did caused the D_H of the aggregates of $\mathbf{2V'}^{2(\bullet+)}$ and $(\mathbf{2V'}^{2(\bullet+)})_2\subset(CB[8])_2$ to decrease continually, but at this low concentration, the D_H was still as high as 70 nm, again supporting the strong stacking tendency.

3 Conclusions

In summary, we have synthesized a series of water-soluble linear di- and triviologen molecules and revealed that the molecules, in their radical cation state, folded into pleated folded conformations in water as highly stable foldamer dimers. The foldamer dimers produce strong absorption of trisradical cations of viologen and also further stack to afford large nanoscale particles. Adding CB[7] break the particles and foldamer dimers as a result of its encapsulation for the viologen radical cation, whereas the addition of CB[8] causes the decomposition of the particles and foldamer dimers through encapsulating the dimers of the viologen radical cation unit. This study shows that, although the folding of the linear viologen molecules in its radical cation state is similar to that revealed in acetonitrile in the literation, the aggregation of the resulting foldamer dimers is much stronger in water, which should be considered in the future for the design of viologen radical cation-based supramolecular architectures in water.

4 Experimental section

4.1 Materials and general methods

Chemicals including compound **1V**•2Cl were purchased as reagent grade and employed without further purification. Compounds **1**～**3**[9] and **4**～**5**[20] were all prepared according to reported procedures.

1,1''-(1,4-Phenylenebis(methylene))bis(([4,4'-bipyridin]-1-ium))hexafluorophosphate, 1,1'-bis(4-([4,4'-bipyridin]-1-ium-1-ylmethyl)benzyl)-[4,4'-bipyridine]-1,1'-diium-

hexafluorophosphate[9] and 1,1''-(1,4-phenylenebis-(methylene))-bis-(([4,4'-bipyridin]-1-ium)) hexafluorophosphate[13] were prepared according to reported procedures.

^{1}H NMR and ^{13}C NMR spectra were recorded by Bruker AVANCE III HD 400 MHz (100 MHz) instrument, and were internally referenced to residual solvent signals (^{1}H NMR: D_2O referenced at δ 4.79). High-resolution mass spectra (HRMS) were recorded on a Bruker McriOTOF11 analyzer. UV/vis/NIR spectra were recorded with a PerkinElmer LAMBDA 650 UV/Vis/NIR spectrometer. Dynamic light scattering (DLS) experiments were conducted on a Malvern Zetasizer Nano ZS90 using a monochromatic coherent He-Ne laser (633 nm) as the light source and a detector that detected the scattered light at an angle of 90°.

4.2 Synthesis

4.2.1 **2V**•4Cl

CH_3I (1.0 mL, 16.1 mmol) was added to a solution of 1,1''-(1,4-phenylenebis(methylene))bis(([4,4'-bipyridin]-1-ium)) hexafluorophosphate (706 mg, 1.0 mmol) in *N*,*N*-dimethylformamide (DMF) (10 mL) in a tube at room temperature, then the mixture was sealed and heated to 80 ℃ for 12 h. The reaction mixture was cooled to room temperature. A solution of TBACl (5.54 g, 20.0 mmol) in CH_3CN (10 mL) was slowly added dropwise the cooled mixture, along with yellow precipitate forming immediately. The mixture was heated up to 80 ℃ again for 6 h and left overnight for cooling. The precipitate was filtered off, washed with CH_3CN and Et_2O and dried under vacuum. The crude product was recrystallized by water and CH_3CN (V∶V=1∶1～1∶2) to afford **2V**•4Cl as a light-yellow solid (570 mg, 97 %). m.p.＞300 ℃ (dec.). ^{1}H NMR (400 MHz, D_2O) δ: 9.18 (d, J=4.0 Hz, 4H), 9.05 (d, J=8.0 Hz, 4H), 8.56 (d, J=8.0 Hz, 4H), 8.51 (d, J=8.0 Hz, 4H), 7.64 (s, 4H), 5.99 (s, 4H), 4.50 (s, 6H); ^{13}C NMR (100 MHz, D_2O) δ: 150.7, 149.7, 146.4, 145.7, 134.1, 130.4, 127.3, 126.8, 64.2, 48.4. HRMS (ESI) calcd for $C_{30}H_{30}N_4P_3F_{18}$ [M－4Cl＋3(PF_6)]$^+$ 881.1390, found 881.1393.

4.2.2 **3V**•6Cl

CH_3I (1.0 mL, 16.1 mmol) was added to a solution of 1,1'-bis(4-([4,4'-bipyridin]-1-ium-1-ylmethyl)benzyl)-[4,4'-bipyridine]-1,1'-diium hexafluorophosphate (1257 mg, 1.0 mmol) in DMF (10 mL) in a tube at room temperature, then the mixture was sealed and heated to 80 ℃ for 12 h. The reaction mixture was cooled to room temperature. A solution of TBACl (5.54 g, 20.0 mmol) in CH_3CN (10 mL) was slowly added dropwise to the cooled mixture, along with orange precipitate forming immediately. The mixture was heated up to 80 ℃ again for 6 h and left overnight for cooling. The precipitate was filtered off, washed with CH_3CN and Et_2O and dried under vacuum. The crude product was recrystallized by water and CH_3CN (V∶V=1∶1～1∶2) to afford **3V**•6Cl as an orange solid (874 mg, 95%). m.p.＞300 ℃ (dec.). ^{1}H NMR (400 MHz, D_2O) δ: 9.21 (d, J=4.0 Hz, 8H), 9.08 (d, J=8.0 Hz, 4H), 8.59 (d, J=4.0 Hz, 8H), 8.55 (d, J=4.0 Hz, 4H), 7.67 (s, 8H), 6.02 (s, 8H), 4.53 (s, 6H); ^{13}C NMR (100 MHz, D_2O) δ: 150.6, 150.4, 149.7, 146.4, 145.7, 134.1,134.0, 130.5, 127.5, 127.4, 126.8, 64.2, 48.5. HRMS (ESI) calcd for $C_{48}H_{46}N_6P_4F_{24}$ [M － 6Cl ＋ 4(PF_6)]$^{2+}$ 643.1170, found 643.1169.

4.2.3 **2V'**•4Cl

CH_3I (1.0 mL, 16.1 mmol) was added to a solution of 1,1''-(1,4-phenylenebis(methylene))-bis-(([4,4'-bipyridin]-1-ium)) hexafluorophosphate (678 mg, 1.0 mmol) in DMF (10 mL) in a tube at room temperature, then the mixture was sealed and heated to 80 ℃ for 12 h. The reaction mixture was cooled to room temperature. A solution of TBACl (5.54 g, 20.0 mmol) in CH_3CN (10 mL) was slowly added dropwise the cooled mixture, along with orange precipitate forming immediately. The mixture was heated up to 80 ℃ again for 6 h and left overnight for cooling. The precipitate was filtered off, washed with CH_3CN and Et_2O and dried under vacuum. The crude product was recrystallized by water and CH_3CN (V∶V=1∶1～1∶2) to afford **2V'**•4Cl as a yellow solid (538 mg, 96%). m.p. ＞300 ℃ (dec.). ^{1}H NMR (400 MHz, D_2O) δ: 9.57 (d, J=4.0 Hz, 4H), 9.16 (d, J=4.0 Hz, 4H), 8.86 (d, J=4.0 Hz, 4H), 8.68 (d, J=8.0 Hz, 8H), 8.31 (s, 4H), 4.58 (s, 6H); ^{13}C NMR (100 MHz, D_2O) δ: 151.9, 149.4, 146.5, 145.7, 144.4, 127.4, 127.0, 126.9, 48.6. HRMS (ESI) calcd for $C_{28}H_{26}N_4P_3F_{18}$ [M－4Cl＋3(PF_6)]$^+$ 853.1077, found 853.1075.

Supporting Information Supplemental results for ^{1}H NMR titration experiments, UV/Vis/NIR dilution experiments, dynamic light scattering (DLS) experiments and NMR spectra of oligoviologens. The Supporting Information is available free of charge via the Internet at http://sioc-journal.cn/.

References

[1] Creighton, T. E. *Proteins*: *Structures and Molecular Principles*, 2nd ed., Freeman, New York, **1993**.

[2] Saenger, W. *Principles of Nucleic Acid Structure*, Springer-Verlag, New York, **1984**.

[3] (a) Gellman, S. H. *Acc. Chem. Res*. **1998**, *31*, 173.
(b) Hill, D. J.; Mio, M. J.; Prince, R. B.; Hughes, T. S.; Moore, J. S. *Chem. Rev*. **2001**, *101*, 3893.
(c) Huc, I. *Eur. J. Org. Chem*. **2004**, *1*, 17.
(d) Gong, B. *Acc. Chem. Res*. **2008**, *41*, 1376.
(e) Li, X.; Wu, Y.-D.; Yang, D. *Acc. Chem. Res*. **2008**, *41*, 1428.
(f) Juwarker, H.; Suk, J.; Jeong, K.-S. *Chem. Soc. Rev*. **2009**, 38, 3316.
(g) Gan, Q.; Wang, Y.; Jiang, H. *Curr. Org. Chem*. **2011**, *15*, 1293.
(h) Zhao, Y.; Cho, H.; Widanapathirana, L.; Zhang, S. *Acc. Chem. Res*. **2013**, *46*, 2763.
(i) Nair, R. V.; Vijayadas, K. N.; Roy, A.; Sanjayan, G. J. *Eur. J. Org. Chem*. **2014**, *35*, 7763.
(j) Huo, Y.-P.; Zeng, H.-Q. *Acc. Chem. Res*. **2016**, *49*, 922.
(k) Shigeno, M.; Kushida, Y.; Yamaguchi, M. *Chem. Commun*. **2016**, *52*, 4955.
(l) Zheng, D.; Yu, C.-Y.; Zheng, L.; Zhan, Y.-L.; Jiang, H. *Chin. Chem. Lett*. **2020**, *31*, 673.

[4] (a) Juwarker, H.; Jeong, K.-S. *Chem. Soc. Rev*. **2010**, *39*, 3664.
(b) Ferrand, Y.; Huc, I. *Acc. Chem. Res*. **2018**, *51*, 970.

(c) Zhao, Y. *Curr. Opin. Colloid Interface Sci.* **2007**, *12*, 92.
[5] (a) Xin, P.-Y.; Zhu, P.-P.; Su, P.; Hou, J.-L.; Li, Z.-T. *J. Am. Chem. Soc.* **2014**, *136*, 1307.
(b) Zhang, D.-W.; Wang, H.; Li, Z.-T. *Prog. Chem*. **2020**, *32*, 1665.
(c) Lang, C.; Li, W.-F.; Dong, Z.-Y.; Zhang, X.; Yang, F.-H.; Yang, B.; Deng, X.-L.; Zhang, C.-Y.; Xu, J.-Y.; Liu, J.-Q. *Angew. Chem.*, *Int. Ed*. **2016**, *55*, 9723.
(d) Chen, F.; Shen, J.; Li, N.; Roy, A.; Ye, R.-J.; Ren, C.-L.; Zeng, H.-Q. *Angew. Chem.*, *Int. Ed.* **2020**, *59*, 1440.
[6] (a) Khan, A.; Kaiser, C.; Hecht, S. *Angew. Chem.*, *Int. Ed.* **2006**, *45*, 12, 1878.
(b) Zhang, K.-D.; Zhao, X.; Wang, G.-T.; Liu, Y.; Zhang, Y.; Lu, H.-J.; Jiang, X.-K.; Li, Z.-T. *Angew. Chem*., *Int. Ed.* **2011**, *50*, 9866.
(c) Chen, L.; Wang, H.; Zhang, D.-W.; Zhou, Y.-M.; Li, Z.-T. *Angew. Chem*., *Int. Ed.* **2015**, *54*, 4028.
(d) Wang, Y.; Bie, F.-S.; Jiang, H. *Org. Lett.* **2010**, *12*, 3630.
(e) Parks, F. C.; Liu, Y.; Debnath, S.; Stutsman, S. R.; Raghavachari, K.; Flood, A. H. *J. Am. Chem. Soc.* **2018**, *140*, 17711.
(f) Pramanik, S.; Kauffmann, B.; Hecht, S.; Ferrand, Y.; Huc, I. *Chem. Commun.* **2021**, *57*, 93.
[7] (a) Stone, M. T.; Moore, J. S. *Org. Lett.* **2004**, *6*, 469.
(b) Sinkeldam, R. W.; van Houtem, M. H. C. J.; Pieterse, K.; Vekemans, J. A. J. M.; Meijer, E. W. *Chem.-Eur. J*. **2006**, *12*, 6129.
(c) Gillies, E. R.; Deiss, F.; Staedel, C.; Schmitter, J.-M.; Huc, I. *Angew. Chem.*, *Int. Ed.* **2007**, *46*, 4081.
(d) Wang, Y.; Li, F.; Han, Y.-M.; Wang, F.-Y.; Jiang, H. *Chem. Eur. J.* **2009**, *15*, 9424.
(e) Suk, J.-M.; Jeong, K.-S. *J. Am. Chem. Soc.* **2008**, *130*, 11868.
(f) Zhang, P.; Wang, Z.-K.; Zhang, L.; Wang, H.; Zhang, D.-W.; Hou, J.-L.; Li, Z.-T. *Chin. J. Chem*. **2016**, *34*, 678.
(g) Shang, J.; Zhao, W.; Li, X.-C.; Wang, Y.; Jiang, H. *Chem. Commun*. **2016**, *52*, 4505.
(h) Ikkanda, B. A.; Iverson, B. L. *Chem. Commun.* **2016**, *52*, 7752.
(i) Borissov, A.; Marques, I.; Lim, J. Y. C.; Felix, V.; Smith, Ma. D.; Beer, P. D. *J. Am. Chem. Soc.* **2019**, *141*, 4119.
[8] (a) Chen, L.; Wang, H.; Zhang, D.-W.; Zhou, Y.-M.; Li, Z.-T. *Angew. Chem*., *Int. Ed.* **2015**, *54*, 4028.
(b) Zhang, Y.-C.; Zhang, D.-W.; Wang, H.; Zhou, Y.-M.; Li, Z.-T. *Polym. Chem*. **2015**, *6*, 4404.
(c) Chen, L.; Wang, H.; Zhang, D.-W.; Zhou, Y.-M.; Li, Z.-T. *Tetrahedron* **2017**, *73*, 1841.
(d) Qi, Q.; Yang, B.; Xi, C.-G.; Yang, X.-R.; Zhang, D.-W.; Liu, S.-M.; Li, Z.-T. *ChemistrySelect* **2016**, *1*, 6792.
[9] Wang, Y.-P.; Frasconi, M.; Liu, W.-G.; Liu, Z.-C.; Sarjeant, A. A.; Nassar, M. S.; Botros, Y. Y.; Goddard, W. A.; Stoddart, J. F. *J. Am. Chem. Soc*. **2015**, *137*, 876.
[10] (a) Zhang, D.-W.; Tian, J.; Chen, L.; Zhang, L.; Li, Z.-T. *Chem. Asian J*. **2015**, *10*, 56.
(b) Chen, L.; Zhang, Y.-C.; Wang, W.-K.; Tian, J.; Zhang, L.; Wang, H.; Zhang, D.-W.; Li, Z.-T. *Chin. Chem. Lett*. **2015**, *26*, 811.
(c) Zhou, X.-H.; Fan, Y.; Li, W.-X.; Zhang, X.; Liang, R.-R.; Lin, F.; Zhan, T.-G.; Jiecheng Cui, J.; Liu, L.-J.; Zhao, X. Zhang, K.-D. *Chin. Chem. Lett.* **2020**, *31*, 1757.
[11] Wang, Y.-P.; Frasconi, M.; Liu, W.-G.; Sun, J.-L.; Wu, Y.-L.; Nassar, M. S.; Botros, Y. Y.; Goddard, W. A.; Wasielewski, M. R.; Stoddart, J. F. *ACS Cent. Sci.* **2016**, *2*, 89.
[12] Zhou, C.; Tian, J.; Wang, J.-L.; Zhang, D.-W.; Zhao, X.; Liu, Y.; Li, Z.-T. *Polym. Chem*. **2014**, *5*, 341.
[13] Liu, H. *Supramol. Chem.* **2019**, *31*, 451.
[14] (a) Liu, X.-B.; Lin, J.-L.; Wang, H.; Zhang, D.-W.; Li, Z.-T. *Chin. J. Org. Chem*. **2020**, *40*, 663 (in Chinese)
(刘旭波, 林佳乐, 王辉, 张丹维, 黎占亭, 有机化学, **2020**, *40*, 663.)
(b) Tian, X.; Zuo, M.; Niu, P.; Wang, K.; Hu, X. *Chin. J. Org. Chem.* **2020**, *40*, 1823 (in Chinese).
(田雪琪, 左旻瓒, 牛蓬勃, 王开亚, 胡晓玉, 有机化学, **2020**, *40*, 1823.)
[15] (a) Correia, H. D.; Chowdhury, S.; Ramos, A. P.; Guy, L.; Demets, G. J.-F.; Bucher, C. *Polym. Int.* **2019**, *68*, 572.
(b) Zhou, J.; Hou, S.; Zhang, J.; Chen, Y.; Chen, H.; Tan, Y. *Chin. Chem. Lett.* **2021**, *32*, 725.
(c) Ong, W.; Gomez-Kaifer, M.; Kaifer, A. E. *Org. Lett.* **2002**, *4*, 1791.
[16] Yang, B.; Zhang, J.-W.; Yu, S.-B.; Wang, Z.-K.; Zhang, P.-Q.; Yang, X.-D.; Qi, Q.-Y.; Yang, G.-Y.; Ma, D.; Li, Z.-T. *Sci. China Chem.* **2021**, *64*, 1228.
[17] (a) Yin, Z.; Song, G.; Jiao, Y.; Zheng, P.; Xu, J.-F.; Zhang, X. *CCS Chem.* **2019**, *1*, 335.
(b) Ji, Q.; Fan, L.; Liu, S.; Ye, H.; Xiang, S.; Wang, P. *Chin. Chem. Lett*. **2021**, 10.1016/j.cclet.2021.05.036.
[18] Geuder, W.; Hunig, S.; Suchy, A. *Tetrahedron* **1986**, *42*, 1665.
[19] Yang, B.; Yu, S.-B.; Wang, H.; Zhang, D.-W.; Li, Z.-T. *Chem. Asian J.* **2018**, *13*, 1312.

(Lu, Y.)

